Available online at www.sciencedirect.com

SciVerse ScienceDirect

Journal of the European Ceramic Society 32 (2012) 2513–2518

www.elsevier.com/locate/jeurceramsoc

Electrically conductive silicon carbide with the addition of Ti–NbC

Františka Frajkorová *, Miroslav Hnatko, Zoltán Lenčéš, Pavol Šajgalík

Institute of Inorganic Chemistry, Slovak Academy of Sciences, Dúbravská cesta 9, SK-84536 Bratislava, Slovak Republic

Received 28 September 2011; received in revised form 15 February 2012; accepted 27 February 2012
Available online 21 March 2012

Abstract

The work deals with the preparation of dense SiC based ceramics with high electrical conductivity. SiC samples with different content of conductive Ti–Nb–Si–C–O based phase were hot pressed at 1820 °C for 1 h in Ar atmosphere under mechanical pressure of 30 MPa. The conductive phase is a mixture of 50 wt% Ti–NbC (molar ratio of Ti/NbC is 1:1.8) and 50 wt% eutectic composition of Y_2O_3–SiO_2. Composite with 30% of conductive Ti–Nb–Si–C–O phase showed the highest electrical conductivity 28.4 S mm^{-1}, while the good mechanical properties of SiC matrix were preserved (fracture toughness K_{IC} = 5.4 MPa m$^{1/2}$ and Vickers hardness 17.8 GPa).

The obtained results show that the developed additive system is suitable for the preparation of SiC-based composite with sufficient electrical conductivity for electric discharge machining.
© 2012 Elsevier Ltd. All rights reserved.

Keywords: Hot-pressing; Composites; Electrical conductivity; Hardness; Carbides; Silicides

1. Introduction

Silicon carbide (SiC) is a promising material for structural and electronic applications owing to its excellent oxidation resistance, high mechanical strength at elevated temperature, high hardness, high corrosion resistance, high thermal conductivity and high thermal shock resistance.[1–3]

SiC ceramics are known as very difficult to machine materials.[4] The main factors that cause SiC ceramics to be hard to shape are their high hardness, high strength and brittleness. Diamond grinding is one of the commonly used techniques for SiC ceramics, but it is a costly process with limitation on the complexity of the final shapes. One way to solve this problem was to add electroconductive phases, such as $MoSi_2$[5,6] and Ti–NbC[7] to extensively resistive SiC ceramics in large quantities for electric discharge machining (EDM). However, the addition of large amount of secondary phases leads to the degradation of high-temperature stability of SiC ceramics. EDM enables to machine extremely hard materials and complex shapes can be produced with high precision. Therefore, EDM is a potential and attractive technology for the machining of ceramics, providing that these materials have a sufficiently high electrical conductivity. A minimum electrical conductivity of 10^{-3} S mm^{-1} is considered as a limit for EDM.[8]

SiC is a semiconductor with a large bandgap ranging from 2.4 eV (β-SiC) to 3.4 eV (2H-SiC) according to the polytype.[9] However, a number of experimental results showed that impurity doping in SiC has led to the wide range of electrical conductivity (10^{-4}–10^{-16} S mm^{-1}) measured at the room temperature.

The main goal of this work was the preparation of dense SiC-based composite with high electrical conductivity and maintaining the good mechanical properties of the original SiC ceramics. Liquid phase sintering was selected for densification and the goals were achieved by two steps. First the Y_2O_3–SiO_2–NbC–Ti additive system was studied and characterized (details of preparation of the additive system is described in Ref. 7). In the second step the electroconductive SiC composite was prepared by addition of the electroconductive system developed in the first step to the SiC matrix. The present paper is devoted to the second step, i.e. to the fabrication of electroconductive SiC ceramics.

The successful preparation of such composite would extend the application potential of such a composite. The possible applications of electroconductive SiC ceramics could be widened, e.g.

* Corresponding author. Tel.: +421 259410443; fax: +421 259410444.
E-mail address: frantiska.frajkorova@savba.sk (F. Frajkorová).

0955-2219/$ – see front matter © 2012 Elsevier Ltd. All rights reserved.
doi:10.1016/j.jeurceramsoc.2012.02.049

Table 1
Chemical composition of the electrically conductive N-phase.

	Composition (wt%)			
	SiO_2	Y_2O_3	Ti	NbC
N-phase	20	30	18	32

as heat exchangers, furnace heating elements, bearings without surface charging, aircraft engine parts, etc., and moreover allows the discharge machining of electrically conductive SiC.

2. Experimental

Commercially available powders of β-SiC (HSC-059, Superior Graphite, USA), SiO_2 (Aerosil OX-50, Degussa, Germany), Y_2O_3 (grade C, H.C. Starck, Germany), Ti (TOHO Titanium Co., Japan) and NbC (Japan New Metals Co., Japan) were used for the starting powders preparation. The SiC-based composites were prepared by the addition of different amount of electrically conductive Ti–Nb–Si–C–O phase (hereafter be cited as "N-phase"[7]) which is a mixture of 50 wt% Ti–NbC (molar ratio of Ti/NbC is 1:1.8) and 50 wt% eutectic composition of Y_2O_3–SiO_2. The chemical composition is listed in Table 1.

The compositions of studied composites and reference SiC materials are listed in Table 2. In the case of composites the ratio SiO_2:Y_2O_3 was 0.39, corresponding to the lowest eutectic temperature $T_E = 1660\,^{\circ}C$ in the binary diagram SiO_2–Y_2O_3, and the ratio Ti:NbC was 1:1.8.[7] The reference material (SiC_{ref}) was prepared for a comparison of the mechanical properties and the electrical conductivity.

The powder mixtures were ball milled in isopropyl alcohol with SiC balls for 24 h. The homogenized suspension was dried and subsequently screened through 71 μm sieve in order to avoid large hard agglomerates. The pre-pressed pellets were hot pressed according to the following regime: 1500 °C/1 h + 1820 °C/1 h in Ar atmosphere under 30 MPa pressure. The reference material was hot pressed at 1820 °C for 1 h in Ar atmosphere under 30 MPa. The densities of the samples were measured by Archimedes method in mercury. The theoretical densities were calculated according to the rule of mixtures. The microstructures were observed by scanning electron microscopy (Zeiss, EVO 40HV, Germany). The elemental analysis of crystalline phases was examined by EDX. For this purpose the sintered samples were cut and polished. The crystalline phases present in the ground samples were identified using X-ray diffraction (XRD) (STOE Stadi-P, Germany, Co Kα radiation). The electrical conductivity measurement was performed by four-probe method. The X-ray microtomography (Nanotom 180) was used to observe the distribution of Ti and Nb particles in the composite. Vickers hardness and fracture toughness were measured using Leco hardness tester (LV-100, Leco Co., USA) by indentation method with a load of 9.8 N and 98 N, respectively.

Table 2
Chemical composition of composites and reference material.

Sample	Composition (wt%)					
	SiC	SiO_2	Y_2O_3	Ti	NbC	AlN
SiC5	90	2	3	1.8	3.2	–
SiC10	80	4	6	3.6	6.4	–
SiC20	60	8	12	7.2	12.8	–
SiC30	40	12	18	10.2	19.8	–
SiC_{ref}	90.7	–	3.9	–	–	5.4

3. Result and discussion

3.1. XRD phase analysis of the samples

The phase composition of samples sintered at 1820 °C is summarized in Table 3 together with the weight loss data and their densities.

From the results listed in Table 3 it is obvious that the weight loss of the composites after sintering increases linearly with the addition of N-phase. It can be assumed that the weight loss is mainly related to the reduction of SiO_2 to gaseous products (e.g. SiO), because the portion of SiO_2 in the starting mixture is almost identical with the observed weight loss of the composites (Table 3). This assumption confirms the results of XRD phase analysis. In the composites with 5–20 wt% of N-phase (SiC5, SiC10, SiC20) yttrium silicate Y_2SiO_5 was identified, whereby the intensity of its diffractions gradually decreases with the increasing portion of N-phase. β-SiC was detected as a majority phase in the mentioned composites, together with the minority NbC and TiC phases. In the composite with 30 wt% of N-phase (SiC30) both β and α modifications of SiC have been detected as a majority phases, and neither yttrium silicate, nor SiO_2 were observed. The minority phases were the carbides of niobium and titanium (NbC, TiC) and their silicides (Nb_5Si_3, Ti_5Si_3). The silicides were not confirmed in the composites with 5–20 wt% of N-phase, but it does not exclude their presence, since their content may be below the detection limit of XRD analysis. The XRD analysis of SiC_{ref} shows the presence of β-SiC, α-SiC, $Y_2Si_2O_7$ and $Y_{10}Al_2Si_3O_{18}N_4$.

3.2. Microstructure

The results of SEM analysis of the polished surfaces of the composites with 5–30 wt% of the conductive N-phase are shown in Fig. 1.

The micrographs show that the amount of pores decreases with the increasing proportion of N-phase. This is in accordance with the observed increasing density (Table 3) with the rising N-phase content. However, we must keep in mind that also the theoretical density increases from SiC5 to SiC30 samples, because the amount of heavy elements (Ti, Nb) also increases and the measured density values do not reflect the real porosity. Moreover, the calculation of the theoretical density from the volume fraction of various phases in the starting mixture can be misleading, because the final phase composition after sintering is different. The porosity of the composites shown in Fig. 1 was estimated on the basis of the area of the pores in the microphotographs and is 47%, 34%, 28% and 16% for samples

Table 3
Mass changes, densities and phase composition of composites and reference material after sintering at 1820 °C.

Sample	Mass changes (%)	Density (g cm^{-3})	Phase composition
SiC5	−4.1	2.14	β-SiC, Y_2O_3, Y_2SiO_5, NbC, TiC
SiC10	−4.8	2.62	β-SiC, Y_2O_3, Y_2SiO_5, NbC, TiC
SiC20	−9.8	3.53	β-SiC, Y_2O_3, Y_2SiO_5, NbC, TiC
SiC30	−12.9	3.69	β-SiC, α-SiC, C (graphite), $C_2Nb_{0.9}Ti_{1.1}$, NbC, Nb_5Si_3, Ti_5Si_3, $Y_3Si_2C_2$, Y_2O_3, TiC
SiC_{ref}	−10	3.32	β-SiC, α-SiC, $Y_2Si_2O_7$, $Y_{10}Al_2Si_3O_{18}N_4$

SiC5, SiC10, SiC20 and SiC30, respectively. The decrease of the porosity is accompanied by the significant grain size reduction, from 5 μm in the case of the composite SiC5 to 1 μm grain size in the composite SiC30. The reduction of the grain size is related to the β → α-SiC phase transformation that was also confirmed by the results of XRD phase analysis of the composites (Table 3). While in the case of composites SiC5–SiC20 cubic β-SiC was detected, in the composite SiC30 also the hexagonal α-SiC was observed. One can suppose that in sample SiC30 larger amount of temporary liquid phase (mainly consisting of N-phase) was present at 1820 °C and the β → α-SiC phase transformation through solution-reprecipitation process reached a higher degree. The growth of hexagonal α-SiC plates (preferential growth in a direction of *a*-axis) is slower than that of cubic β-SiC at this sintering temperature.[10] Moreover, the grain growth is inhibited also by the carbides of titanium and niobium which crystallize from the melt in the composite SiC30. For the comparison the microstructures of reference material SiC_{ref} are shown in Fig. 2. The particle size of α-SiC in the sample SiC30 is close to the particle size of SiC_{ref}.

Although the presence of remaining porosity, the amount and connection of the phase at the grain boundaries, as well as its chemical composition should be sufficient for increasing the electrical conductivity of prepared composites.

3.3. Mechanical properties

Fig. 3 shows the dependence of fracture toughness (K_{IC}) and hardness (*HV*) of the composites on the conductive phase content. For a comparison the properties of reference material SiC_{ref} are also shown. In the case of composites it is obvious that with increasing conductive phase content also the hardness increases.

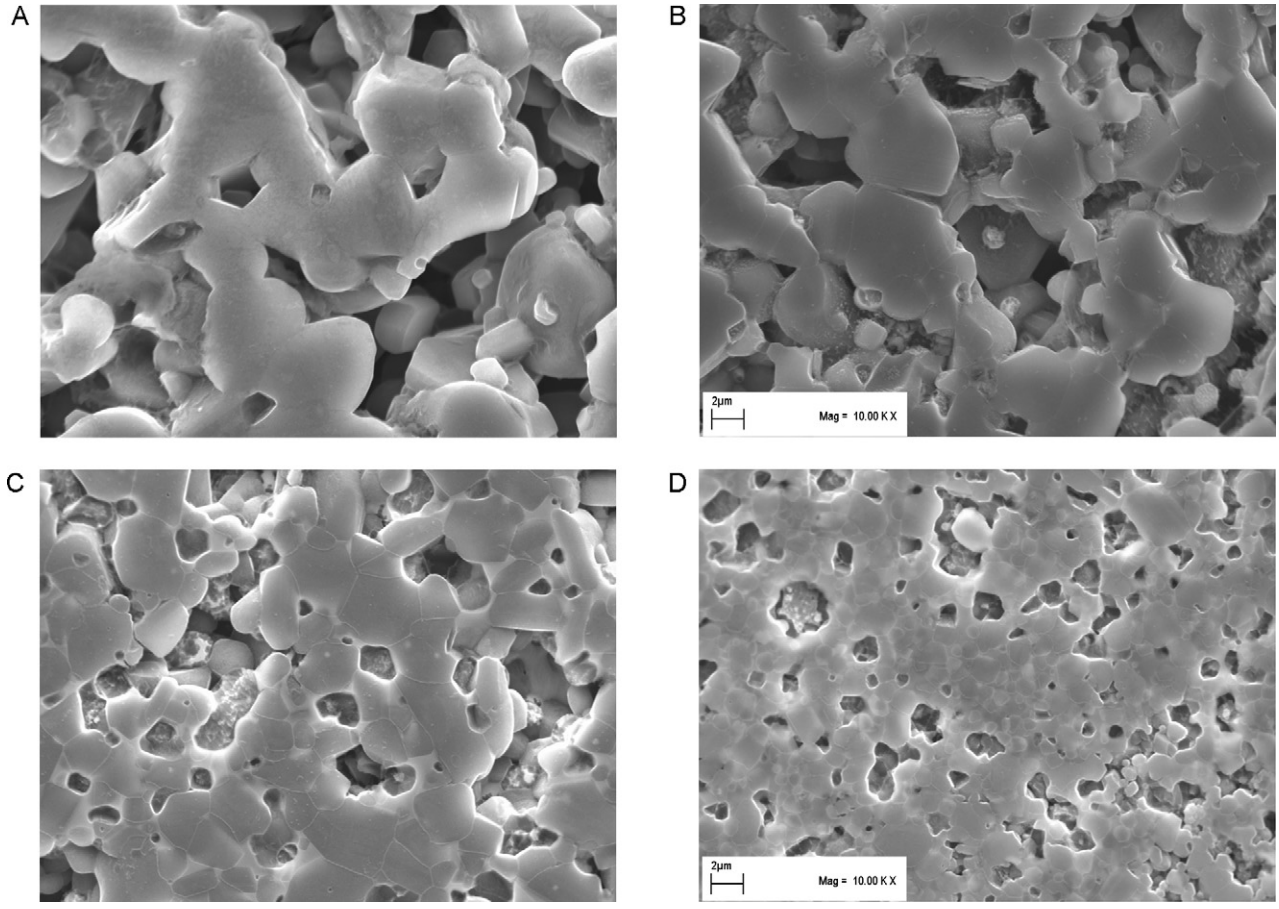

Fig. 1. The microstructures of SiC-based composites with different content of conductive N-phase (magnification 10,000×). (a) SiC5, (b) SiC10, (c) SiC20 and (d) SiC30.

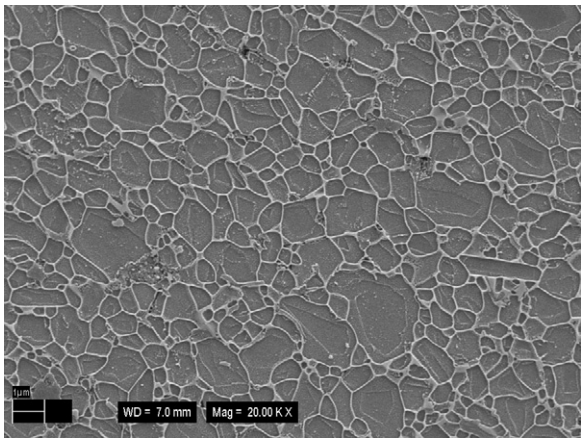

Fig. 2. The microstructure of reference material SiC_{ref}.

It is related to the increasing content of phases with high hardness (TiC, NbC) in the composites and also to the character of the microstructure. In accordance with the Hall–Petch phenomenon, the hardness of fine-grained material is higher than the coarse-grained ones. The porosity (P) of the samples also affects the hardness (H) of the material, which decreases exponentially with the increase of porosity ($H \sim e^{-bP}$).[11]

The low hardness of the samples SiC5 (1.1 GPa) and SiC10 (3.4 GPa) is due to the coarse-grained microstructure (5 μm the average grain size) and the high porosity. Remarkable increase of the hardness occurs in the case of the sample SiC20 (15.2 GPa), which has a significantly different microstructure compared to the previously mentioned composites SiC5 and SiC10. Sample SiC30 has the highest hardness (17.8 GPa). Compared with the reference material SiC_{ref} the value is lower by 2.8 GPa. In terms of the amount of liquid phase at the grain boundaries, which generally degrades the hardness of SiC-based materials prepared by liquid phase sintering, even more significant difference in hardness values of the sample SiC30 (30 wt% of SiO_2 and Y_2O_3 sintering additives) would be expected compared with SiC_{ref} (10 wt% of AlN and Y_2O_3 sintering additives). The observed high hardness of SiC30 sample among the composites is due

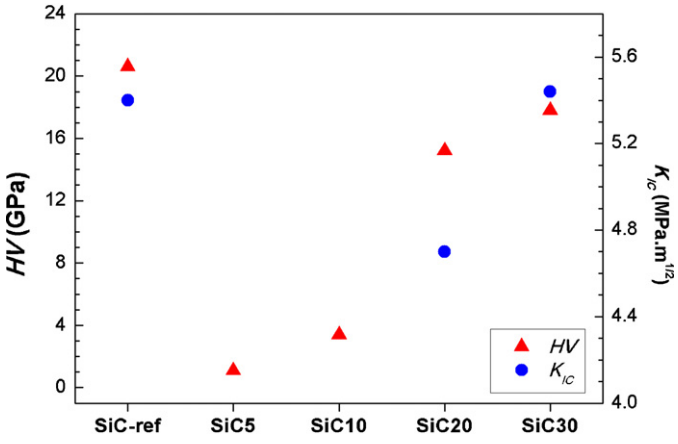

Fig. 3. The hardness (HV) and indentation fracture toughness (K_{IC}) of the reference material (SiC-ref) and SiC composites depending on the addition of the conductive phase.

to the lowest porosity, the presence of hard TiC and NbC, and also due to the significant reduction of liquid phase (reduction of SiO_2) and the phase composition change of the grain boundary phase. Yttrium silicate with a hardness of only 4–5 GPa was not detected in the sample SiC30. It is expected that by the optimization of the sintering conditions, or by modifying the chemical composition of the starting mixture of sample SiC30 in order to reduce its porosity we can achieve even higher values of hardness.

The indentation fracture toughness K_{IC} was measured only on the composites SiC20 (4.7 MPa m$^{1/2}$) and SiC30 (5.4 MPa m$^{1/2}$), because the other composites had a high porosity. The fracture toughness of the sample SiC30 was comparable to the reference material (K_{IC} (SiC_{ref}) = 5.4 MPa m$^{1/2}$). The microstructure and crack propagation in the composites SiC20, SiC30 and reference material SiC_{ref} are shown in Fig. 4a–c. The similar crack path with obvious crack deflection in samples SiC30 and SiC_{ref} explains their similar fracture toughness. In both cases there is an intergranular fracture which propagates along the SiC grains.

In the case of composites the fracture toughness increases with the addition of conductive Nb–Ti–C phase. The increasing content of metallic phase in a ceramic matrix causes a change of fracture mechanism. The brittle fracture, characteristic for ceramic materials, becomes partially ductile with the addition of a metallic phase. The metal component, characterized by elastic deformation, dissipates the energy of propagating cracks and thereby actually increases the fracture toughness of materials. However, in our case the fracture toughness of the composites had not increased because of the low content of the metallic phase. From Table 3 is evident that in the studied system there are various types of compounds with different coefficients of thermal expansion. Therefore, after the sintering of composites during the cooling process residual stresses are formed in the materials, and these stresses may also affect the deflection and branching of the propagating cracks and thereby influence the mechanical properties of prepared SiC composites.

3.4. Electrical conductivity

The main goal of the work was the preparation of SiC-based composite with sufficiently high electrical conductivity suitable for EDM. As a conductive and sintering additive so called N-phase was used which has an electrical conductivity 238 S mm^{-1}.[7] The optimization of the chemical composition of electrically conductive N-phase (Table 1) is discussed elsewhere.[7] It was expected that the electrically non-conductive SiC systems with the addition of conductive N-phase at the grain boundaries will follow the percolation phenomena and from the certain volume fraction of conductive phase the electrical conductivity of SiC composite significantly increases. However, in our systems the electrical conductivity increases almost linearly with the addition of conductive N-phase and the percolation phenomenon is not significant (Fig. 5). It can be caused by the formation of homogeneously distributed conductive amorphous phase based on Ti–Nb–C–O–(Si) at the grain boundaries. This phase has a lower electrical conductivity than the crystalline silicides and carbides, but higher than SiC does have,[12,13] and

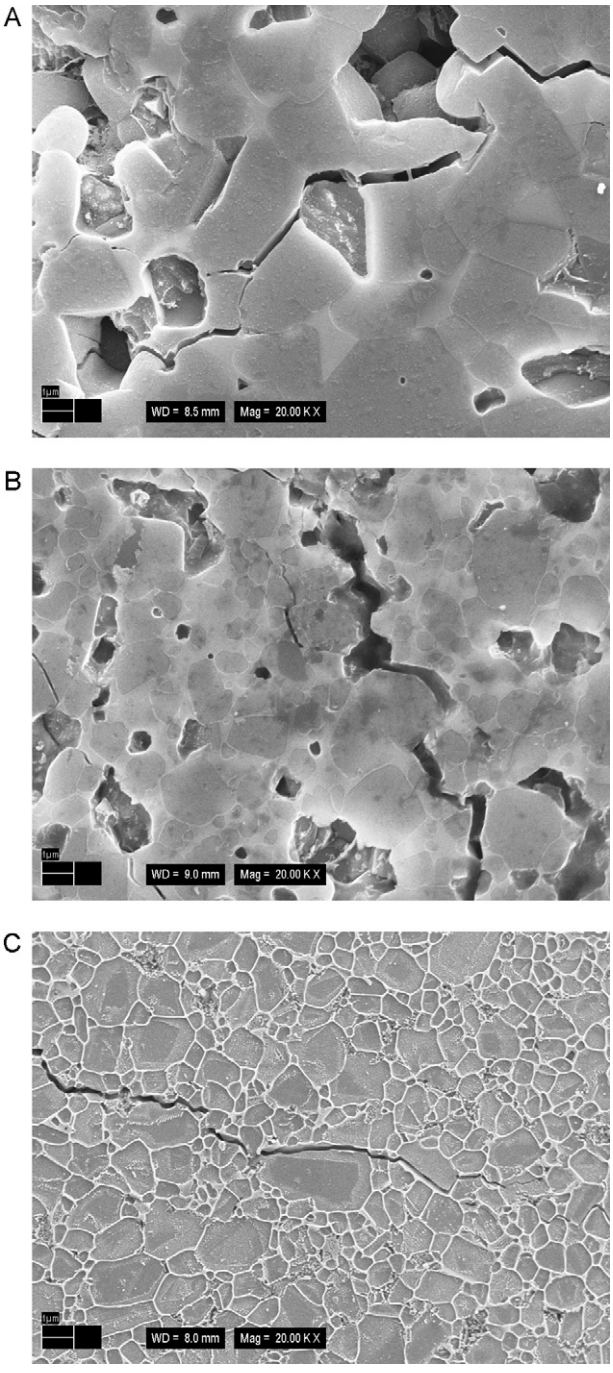

Fig. 4. The crack propagation in the composites (a) SiC20, (b) SiC30 and in the reference material (c) SiC_{ref}.

due to the continuous network formation on the grain boundaries its effect on electrical conductivity of SiC-based composite is remarkable already at low contents. According to the literature, only 5–8 vol% of electrically conductive amorphous phase is necessary to achieve a uniform distribution of this phase at the grain boundaries,[14,15] while for obtaining a similar percolation effect by the addition of discrete crystalline particles about 15–30 vol% of electrically conductive phase is required.[16–18] The critical volume fraction of electrically conductive component increases with its increasing particle size and ~30 vol% is necessary when the particle size of the matrix and conductive component are approximately equal.

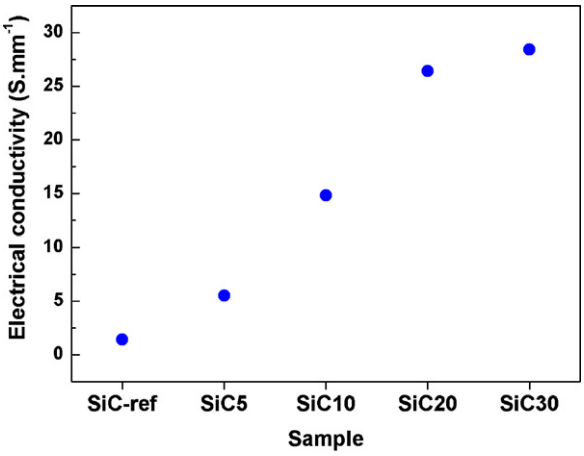

Fig. 5. Electrical conductivities of reference material and SiC composites.

The results shown in Fig. 5 suggest that our case is probably a combination of two mentioned phenomena, i.e. the electrical conductivity of SiC composite is improved by the crystalline silicides and carbides of niobium and titanium which exhibit metallic conductivity,[19] as well as by the amorphous phase based on Ti–Nb–C–O–(Si).[7]

The significant percolation phenomenon is in our case partly inhibited also by the presence of pores. The low electrical conductivity of the samples SiC5 (5.5 S mm^{-1}) and SiC10 (14.8 S mm^{-1}) is mainly caused by the high porosity and low content of conductive phases, which probably do not form a continuous conductive network in these samples. Nevertheless, the conductivity of the sample SiC5 is four times higher compared to the reference material SiC_{ref} (1.4 S mm^{-1}). In the case of sample SiC30 the electrical conductivity had increased by 20 times to 28.4 S mm^{-1}, in comparison to the reference material SiC_{ref}. The higher conductivity of sample SiC30 was achieved by the reduction of porosity and by the change of phase composition, as was shown by the phase analysis (Table 3), which confirms the presence of electroconductive titanium and niobium silicides (Nb_5Si_3, Ti_5Si_3). In other composites with lower N-phase content only carbides were detected. The specific electrical conductivity of silicides (σ (Nb_5Si_3) = 550 S mm^{-1}, σ (Ti_5Si_3/TiSi) = 418 S mm^{-1}) is the order of magnitude higher in comparison with carbides (σ (TiC) = 14.7 S mm^{-1}, σ (NbC) = 13.5 S mm^{-1})[19] and their presence could significantly affect the electrical conductivity of the composite.

The distribution of the phases rich in titanium and niobium (light grey phases) in sample SiC20 are shown in Fig. 6. The images were obtained using XRD microtomograph and provide some idea about the connection of conductive phases. The lighter colour phases are rich in Ti and Nb and form a continuous network. This analysis confirms that the used additive system and processing method can be used for the preparation of SiC-based composites with coherent conductive network rich in titanium and niobium.

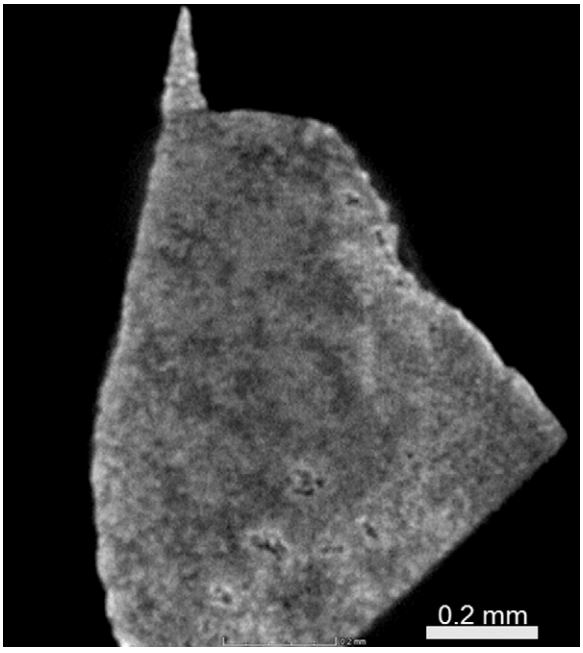

Fig. 6. XRD microtomography of SiC20 composite.

4. Conclusions

Electroconductive SiC composite was prepared by using NbC–Ti–SiO_2–Y_2O_3 additives and hot-pressing at 1820 °C. The partial results can be summarized as follows:

- The conductive N-phase composed of NbC–Ti–SiO_2–Y_2O_3 is a suitable additive for the densification of SiC, because at 1820 °C sufficiently wets the surface of the solid phase (SiC) and the grains of sintered material (SiC) are partially soluble in it what was evidenced by the β → α-SiC phase transformation.
- The highest density of SiC-based composites was achieved in the sample SiC30, i.e. with the addition of 30 wt% conductive N-phase.
- The increasing content of conductive N-phase which contains hard NbC and TiC, leads to the increase of hardness. The highest value of hardness $HV = 17.8$ GPa was obtained for the sample SiC30. The hardness is lower by 2.8 GPa compared with the reference material SiC_{ref}, caused mainly by the higher porosity.
- Carbides crystallize at SiC grain boundaries and thereby inhibit their growth, resulting in finer microstructure and increased hardness (Hall–Petch phenomena).
- The XRD microtomography results showed that the applied additive system and processing method allowed the preparation of SiC-based composites (SiC20 and SiC30) with continuous conductive network rich in titanium and niobium. In the case of the sample SiC30 the electrical conductivity increased 20 times ($\sigma = 28.4$ S mm^{-1}) in comparison with the reference material SiC_{ref}.

Acknowledgements

This work was supported by the Slovak Grant Agency VEGA 2/0036/10 and APVV-0171-06. This publication is the result of the project implementation: High-flow plasma generator based on composite materials for gasification of solid hydrocarbons 26240220054 supported by the Research & Development Operational Programme funded by the ERDF. Authors would like to thank Dr. Peter Švec (Institute of Physics, Slovak Academy of Sciences) for the electrical conductivity measurements.

References

1. Jang BK, Sakka Y. Thermophysical properties of porous SiC ceramics fabricated by pressureless sintering. *Sci Technol Adv Mater* 2007;**8**:655–9.
2. Zawrah MF, El-Gazery M. Mechanical properties of SiC ceramics by ultrasonic nondestructive technique and its bioactivity. *Mater Chem Phys* 2007;**106**:330–7.
3. Horváth E, Zsíros Gy, Tóth AL, Sajó I, Arató O, Pfeifer J. Microstructural characterization of the oxide scale on nitride bonded SiC-ceramics. *Ceram Int* 2008;**34**:151–5.
4. Luis CJ, Puertas I, Villa G. Material removal rate and electrode wear study on the EDM of silicon carbide. *J Mater Process Technol* 2005;**164/165**: 889–96.
5. Zhang X, Lu Z, Jin Z. Electrical resistivity and microstructure of pressureless reactive sintered $MoSi_2$–SiC composite. *Mater Chem Phys* 2004;**86**: 16–20.
6. Sciti D, Silvestroni L, Balbo A, Guicciardi S, Pezzotti G. High-strength and -toughness electroconductive SiC-based composites. *Adv Eng Mater* 2006;**8**:997–1001.
7. Frajkorová F, Hnatko M, Lenčéš Z, Šajgalík P. Model system Y_2O_3–SiO_2–Ti–NbC for liquid phase sintering of SiC with high electrical conductivity. *Ceram Int*, submitted for publication.
8. Konig W, Dauw DF, Levy G, Panten U. EDM-future step towards the machining of ceramics. *Ann CIRP* 1988;**37**:623–31.
9. Persson C, Lindefelt U. Relativistic band structure calculation of cubic and hexagonal SiC polytypes. *J Appl Phys* 1997;**82**:5496–508.
10. Zhan G-D, Mitomo M, Kim Y-W. Microstructural control for strengthening of silicon carbide ceramics. *J Am Ceram Soc* 1999;**82**:2924–6.
11. Wereszczak AA, Lin HT, Gilde GA. The effect of grain growth on hardness in hot-pressed silicon carbides. *J Mater Sci* 2006;**41**:4996–5000.
12. Mathew MT, Ariza E, Rocha LA, Fernandes AC, Vaz F. TiC_xO_y thin films for decorative applications: tribocorrosion mechanisms and synergism. *Tribol Int* 2008;**41**:603–15.
13. Fernandes AC, Carvalho P, Vaz F, Lanceros-Mendez S, Machado AV, Parreira NMG, et al. Property change in multifunctional TiC_xO_y thin films: effect of the O/Ti ratio. *Thin Solid Films* 2006;**515**:866–71.
14. McLachlan DS, Blaszkiewicz M, Newnham RE. Electrical resistivity of composites. *J Am Ceram Soc* 1990;**73**:2187–203.
15. Kawaoka H, Kim YH, Sekino T, Choa YH, Kusunose T, Nakayama T, et al. New approach to provide an electrical conductivity to structural ceramics. *J Ceram Proc Res* 2001;**2**:1–3.
16. Kirkpatrick S. Percolation and conduction. *Rev Mod Phys* 1973;**45**:574–8.
17. Kusy RP. Influence of particle size ratio on the conductivity of aggregates. *J Appl Phys* 1977;**48**:5301–5.
18. Bellosi A, Guicciardi S, Tampieri A. Development and characterization of electroconductive Si_3N_4–TiN composites. *J Eur Ceram Soc* 1992;**9**: 83–93.
19. Capano MA, Patterson JK, Petry L, Solomon JS. Time-dependent characteristics of titanium–silicide contacts to 6H-silicon carbide. *J Electron Mater* 2003;**32**:458–62.